AIAA Guidance, Navigation, and Control Conference and Exhibit
15 - 18 August 2005, San Francisco, California

AIAA 2005-6196

Nonlinear Trajectory Tracking for Fixed Wing UAVs via Backstepping and Parameter Adaptation

Wei Ren*

Department of Electrical and Computer Engineering, Utah State University, Logan, UT, 84322, USA

Ella Atkins†

Space Systems Laboratory, University of Maryland, College Park, MD 20742, USA

Equipping a fixed wing unmanned air vehicle (UAV) with low-level autopilots, we derive high-level velocity and roll angle control laws for the UAV. Backstepping techniques are applied to design the velocity and roll angle control laws from known velocity and heading angle control laws that explicitly account for velocity and heading rate constraints of the UAV. Regarding unknown autopilot constants, a parameter adaptation technique is used to estimate autopilot parameters. Simulation results on a fixed wing UAV are presented to show the effectiveness of our approach.

Nomenclature

x, y	inertial position, m
ψ	heading angle, rad
ϕ	roll angle, rad
v	Airspeed, m/s
h	Altitude, m
α_*	Autopilot Parameters
g	gravitational constant, m/s^2
Subscript	
r	reference
Superscript	
c	command

I. Introduction

ADVANCED control technologies for unmanned air vehicles (UAVs) have received significant attention in recent years. Potential applications of autonomous UAVs in both civilian and military sectors include environment monitoring, search and rescue, communication relays, border patrol, situation awareness, surveillance, and battle damage assessment.

Fully-automating UAVs poses both theoretical and practical challenges.[1] One important research is UAV path planning.[2,3] Another important aspect focuses on trajectory optimization for UAVs.[4,5] In addition, cooperative control of multiple UAVs is also studied extensively in the literature.[6–8]

Effective trajectory tracking algorithms guarantee that a UAV can accurately follow its pre-specified desired trajectory. In addition, the study of nonlinear tracking control techniques for UAVs is essential for the success of cooperative timing (e.g. Refs. 9,10) and formation keeping missions (e.g. Ref. 11). In Ref. 12, velocity and heading control laws that explicitly account for stall conditions, thrust limitations, and saturated

*Assistant Professor, Department of Electrical and Computer Engineering, Utah State University, Email: weiren@ieee.org
†Assistant Professor, Department of Aerospace Engineering, University of Maryland, Email: ella@ssl.umd.edu, Senior Member.

heading rate constraints are designed for small fixed wing UAVs equipped with velocity hold, heading hold, and altitude hold autopilots. In Ref. 12, it is assumed that the autopilot response to heading commands is first order in nature. However, the headings of the UAVs are controlled by their roll motions, which imply that the kinematic model for UAVs should explicitly take into account the roll angle command. In addition, the autopilot constants are generally unknown and depend on specific designs. Using inaccurate autopilot constants in a control law design may result in degraded performance for the UAV. In this paper, we use a more accurate kinematic model that takes into account the roll motion for heading control. We apply backstepping techniques to derive velocity and roll angle control laws. In addition, a parameter adaptation technique is developed for the control law design regarding unknown autopilot constants. This paper is the continuation of the previous work presented in Ref. 12.

II. Problem Statement

Let (x, y), ψ, v, ϕ, and h denote the inertial position, heading angle, velocity, roll angle, and altitude of the UAV respectively. We assume that the UAV is equipped with standard autopilots as described in Ref. 13. The kinematic equations of motion are given by

$$\begin{aligned}
\dot{x} &= v\cos(\psi) \\
\dot{y} &= v\sin(\psi) \\
\dot{\psi} &= g\frac{\tan(\phi)}{v} \\
\dot{v} &= \frac{1}{\alpha_v}(v^c - v), \\
\dot{\phi} &= \frac{1}{\alpha_\phi}(\phi^c - \phi), \\
\ddot{h} &= -\frac{1}{\alpha_{\dot{h}}}\dot{h} + \frac{1}{\alpha_h}(h^c - h),
\end{aligned} \tag{1}$$

where ϕ^c, v^c, and h^c are the commanded roll angle, velocity, and altitude to the autopilots, g is the gravitational constant, and α_* are positive constants.[13,14]

In the following, we assume that an effective altitude controller exists and focus on the design of velocity and roll angle control laws.

Due to the stall conditions, thrust limitations, and roll angle and pitch rate constraints of fixed wing aircraft, the following input constraints are imposed on the UAV:

$$\begin{aligned}
0 < v_{min} \le v \le v_{max} \\
-\phi_{max} \le \phi \le \phi_{max}
\end{aligned} \tag{2}$$

where $\phi_{max} > 0$.

We assume that the desired reference trajectory $(x_r, y_r, \psi_r, v_r, \omega_r)$ generated by a trajectory generator[5] satisfies

$$\begin{aligned}
\dot{x}_r &= v_r\cos(\psi_r) \\
\dot{y}_r &= v_r\sin(\psi_r) \\
\dot{\psi}_r &= \omega_r
\end{aligned} \tag{3}$$

where v_r and ω_r are continuous and satisfy that $\dot{v}_r$ and $\dot{\omega}_r$ are bounded, $\inf_{t\ge 0} v_r(t) > v_{min}$, $\sup_{t\ge 0} v_r(t) < v_{max}$, and $\sup_{t\ge 0} |\omega_r(t)| < \omega_{max}$ with $\omega_{max} > 0$ denoting the heading rate constraint of the UAV.

Transforming the tracking errors expressed in the inertial frame to the UAV frame, the error coordinates[15] become

$$\begin{bmatrix} x_e \\ y_e \\ \psi_e \end{bmatrix} = \begin{bmatrix} \cos(\psi) & \sin(\psi) & 0 \\ -\sin(\psi) & \cos(\psi) & 0 \\ 0 & 0 & 1 \end{bmatrix} \begin{bmatrix} x_r - x \\ y_r - y \\ \psi_r - \psi \end{bmatrix}. \tag{4}$$

Note that the motivation for this transformation is only to simplify the mathematics so that a constrained Lyapunov function can be easily derived.

Accordingly, the tracking error model can be represented as

$$\begin{aligned}\dot{x}_e &= g\frac{\tan(\phi)}{v}y_e - v + v_r\cos(\psi_e)\\ \dot{y}_e &= -g\frac{\tan(\phi)}{v}x_e + v_r\sin(\psi_e)\\ \dot{\psi}_e &= \omega_r - g\frac{\tan(\phi)}{v}.\end{aligned} \tag{5}$$

III. Trajectory Tracking Using Backstepping and Parameter Adaptation Techniques

In Ref. 12, the authors use the following simplified kinematic model for the UAV:

$$\begin{aligned}\dot{x} &= v^c\cos(\psi)\\ \dot{y} &= v^c\sin(\psi)\\ \dot{\psi} &= \frac{1}{\alpha_\psi}(\psi^c - \psi),\end{aligned} \tag{6}$$

where v^c and ψ^c are the commanded velocity and heading to the autopilots and $\alpha_\psi > 0$ is an autopilot constant.

However, the autopilot response to the heading command is not truly first order in reality. As a result, Eq. (1) represents a more accurate model of the UAV equipped with standard autopilots.

Let

$$v_0 = \begin{cases} v_{min}, & \eta_v x_e < \underline{v}\\ v_r\cos(\psi_e) + \eta_v x_e, & \underline{v} \le \eta_v x_e \le \bar{v}\\ v_{max}, & \eta_v x_e > \bar{v}\end{cases}, \tag{7}$$

$$\omega_0 = \begin{cases} \omega_{max}, & -\eta_\omega\sigma_\omega < \underline{\omega}\\ \omega_r + \eta_\omega\sigma_\omega, & \underline{\omega} \le -\eta_\omega\sigma_\omega \le \bar{\omega}\\ -\omega_{max}, & -\eta_\omega\sigma_\omega > \bar{\omega}\end{cases}, \tag{8}$$

where $\underline{v} \triangleq v_{min} - v_r\cos(\psi_e)$, $\bar{v} \triangleq v_{max} - v_r\cos(\psi_e)$, $\underline{\omega} \triangleq \omega_r - \omega_{max}$, $\bar{\omega} \triangleq \omega_r + \omega_{max}$, $\sigma_\omega \triangleq \lambda\psi_e + \frac{y_e}{\sqrt{x_e^2+y_e^2+1}}$, and η_v and η_ω are sufficiently large positive constants expressed precisely in Ref. 12. In Ref. 12, it is shown that $v^c = v_0$ and $\psi^c = \alpha_\psi\omega_0 + \psi$ guarantees that $|x - x_r| + |y - y_r| + |\psi - \psi_r| \to 0$ asymptotically. In addition, v_0 and ω_0 satisfy the following input constraints

$$\begin{aligned}0 < v_{min} \le v_0 \le v_{max}\\ -\omega_{max} \le \omega_0 \le \omega_{max},\end{aligned}$$

which represents the case that the UAV has limited velocity and heading rate constraints.

However, the velocity and heading rate commands (7) and (8) are no longer valid for Eq. (1), where the control commands to the autopilot are the velocity and roll angle commands. In the following, we apply backstepping techniques to derive velocity and roll angle commands.

Note that Eqs. (1) and (5) can be rewritten as

$$\dot{\chi} = f(t,\chi) + g(\chi)\xi \tag{9}$$

$$\dot{\zeta} = \nu, \tag{10}$$

where $\chi = [x_e, y_e, \psi_e]^T$,

$$\xi = \begin{bmatrix} v \\ g\frac{\tan(\phi)}{v}\end{bmatrix}$$

$$\zeta = \begin{bmatrix} v \\ \phi \end{bmatrix}$$

$$f(t,\chi) = \begin{bmatrix} v_r \cos(\psi_e) \\ v_r \sin(\psi_e) \\ \omega_r \end{bmatrix}$$

$$g(\chi) = \begin{bmatrix} -1 & y_e \\ 0 & -x_e \\ 0 & -1 \end{bmatrix}$$

$$\nu = \begin{bmatrix} \nu_v \\ \nu_\phi \end{bmatrix} = \begin{bmatrix} \frac{1}{\alpha_v}(v^c - v) \\ \frac{1}{\alpha_\phi}(\phi^c - \phi) \end{bmatrix}.$$

Assume that ξ is the control input to Eq. (9) and suppose that we have found a control law $\xi^d = [v^d, g\frac{\tan(\phi^d)}{v^d}]^T$ that stabilizes χ. Furthermore, assume that there exists a Lyapunov function V_1 satisfying $\dot{V}_1 \leq -W(\chi)$ with ξ^d as the control input, where $W(\cdot)$ is a positive definite function.

However, ξ is not a true control input in reality, so we will try to design v^c and ϕ^c such that $\xi \rightarrow [v^d, g\frac{\tan(\phi^d)}{v^d}]^T$ in the next step.

Let $\omega = g\frac{\tan(\phi)}{v}$ and $\omega^d = g\frac{\tan(\phi^d)}{v^d}$. Consider a Lyapunov function candidate

$$V_2 = V_1 + \frac{1}{2} z^T z, \tag{11}$$

where

$$z = \xi - \xi^d = \begin{bmatrix} v - v^d \\ \omega - \omega^d \end{bmatrix}. \tag{12}$$

Differentiating Eq. (11), we get that

$$\begin{aligned} \dot{V}_2 &= \frac{\partial V_1}{\partial \chi} f(t,\chi) + \frac{\partial V_1}{\partial \chi} g(\chi)\xi + z^T \dot{z} \\ &= \frac{\partial V_1}{\partial \chi} f(t,\chi) + \frac{\partial V_1}{\partial \chi} g(\chi)[\xi^d + (\xi - \xi^d)] \\ &+ z^T \begin{bmatrix} \dot{v} - \dot{v}^d \\ g\frac{\sec^2(\phi) v\dot{\phi} - \tan(\phi)\dot{v}}{v^2} - \dot{w}^d \end{bmatrix} \\ &= -W(\chi) \\ &+ z^T \left(\begin{bmatrix} \dot{v} - \dot{v}^d \\ g\frac{\sec(\phi)^2 v\dot{\phi} - \tan(\phi)\dot{v}}{v^2} - \dot{w}^d \end{bmatrix} + (\frac{\partial V_1}{\partial \chi} g(\chi))^T \right), \end{aligned}$$

where $\dot{v}^d$ and $\dot{\omega}^d$ represent the time derivative of v^d and ω^d in the case that v^d and ω^d are differentiable. In the case that v^d and ω^d are not differentiable, we let $\dot{\tilde{v}}^d$ and $\dot{\tilde{\omega}}^d$ denote the generalized time derivative of v^d and ω^d respectively and let $\dot{v}^d$ and $\dot{\omega}^d$ represent the minimum norm element of $\dot{\tilde{v}}^d$ and $\dot{\tilde{\omega}}^d$ respectively (see Refs. 16, 17).

Define

$$P = \begin{bmatrix} 1 & 0 \\ -g\frac{\tan(\phi)}{v^2} & g\frac{\sec^2(\phi)}{v} \end{bmatrix}.$$

Letting

$$\begin{bmatrix} \nu_v \\ \nu_\phi \end{bmatrix} = P^{-1} \left(-Kz - (\frac{\partial V_1}{\partial \chi} g(\chi))^T + \begin{bmatrix} \dot{v}^d \\ \dot{\omega}^d \end{bmatrix} \right),$$

we have

$$\begin{aligned} v^c &= \alpha_v \nu_v + v \\ \phi^c &= \alpha_\phi \nu_\phi + \phi. \end{aligned} \tag{13}$$

Given the control command (13), we can see that $\dot{V}_2 = -W(\chi) - z^T K z$, which is negative definite. As a result, it is straightforward to see that the control command (13) guarantees that $|x_e| + |y_e| + |\psi_e| + |v - v^d| + |g\frac{\tan(\phi)}{v} - g\frac{\tan(\phi^d)}{v^d}| \to 0$, which in turn implies that $|x - x_r| + |y - y_r| + |\psi - \psi_r| \to 0$.

Now we need to find v^d and ω^d and a Lyapunov function V such that

$$\dot{V} = \frac{\partial V}{\partial \chi} f(t, \chi) + \frac{\partial V}{\partial \chi} g(\chi) \begin{bmatrix} v^d \\ \omega^d \end{bmatrix}$$

is negative definite.

In Ref. 12 we have shown that

$$V_0(\chi) = \sqrt{\left(\lambda\psi_e + \frac{y_e}{\sqrt{x_e^2 + y_e^2 + 1}}\right)^2 + 1} \tag{14}$$

$$+ k\sqrt{x_e^2 + y_e^2 + 1} - (1 + k) \tag{15}$$

is a constrained Lyapunov function for system $\dot{\chi} = f(t, \chi) + g(\chi)[v, \omega]^T$ with virtual control inputs v and ω given by Eqs. (7) and (8) such that $\dot{V}_0(\chi) \leq -W(\chi)$, where $W(\chi)$ is a continuous positive-definite function, $k > \frac{1}{2}$, $\lambda > \kappa$, where κ is a positive constant expressed precisely in Ref. 12.

Therefore, we have the following lemma.

Lemma III.1 *Let $v^d = v_0$ and $\omega^d = \omega_0$, where v_0 and ω_0 are given by Eqs.* (7) *and* (8)*. The control command* (13) *guarantees that $|x - x_r| + |y - y_r| + |\psi - \psi_r| + |v - v_r| + |g\frac{\tan(\phi)}{v} - \omega_r| \to 0$ asymptotically.*

Proof: Letting $V_1 = V_0(\chi)$ in Eq. (11), we can see that $\dot{V}_2 = -W(\chi) - z^T K z$, which implies that $\chi \to 0$ and $z \to 0$ asymptotically, that is, $|x_e| + |y_e| + |\psi_e| \to 0$ and $|v - v^d| + |g\frac{\tan(\phi)}{v} - \omega^d| \to 0$. The fact that $\chi \to 0$ also implies that $|v^d - v_r| + |\omega^d - \omega_r| \to 0$. Combining the above arguments, we know that $|x - x_r| + |y - y_r| + |\psi - \psi_r| + |v - v_r| + |g\frac{\tan(\phi)}{v} - \omega_r| \to 0$ asymptotically. ■

In reality, the parameter vector $\theta = [\alpha_v, \alpha_\phi]^T$ is unknown and depends on the autopilot design. The commanded velocity v^c and roll angle ϕ^c are given by $v^c = \hat{\alpha}_v \nu_v + v$ and $\phi^c = \hat{\alpha}_\phi \nu_\phi + \phi$, where $\hat{\theta} = [\hat{\alpha}_v, \hat{\alpha}_\phi]^T$ is an estimate of θ.

Let the parameter estimate vector be updated as

$$\dot{\hat{\theta}} = -\Gamma \begin{bmatrix} \nu_v & 0 \\ 0 & \nu_\phi \end{bmatrix} P^T z, \tag{16}$$

where Γ is a diagonal positive definite matrix.

Consider a Lyapunov function candidate

$$V_3 = V_2 + \frac{1}{2}\tilde{\theta}^T \begin{bmatrix} \frac{1}{\alpha_v} & 0 \\ 0 & \frac{1}{\alpha_\phi} \end{bmatrix} \Gamma^{-1} \tilde{\theta}, \tag{17}$$

where $\tilde{\theta} = \theta - \hat{\theta}$.

Differentiating Eq. (17), we get that

$$\begin{aligned} \dot{V}_3 &= -W(\chi) - z^T K z - z^T P \begin{bmatrix} \frac{\nu_v}{\alpha_v} & 0 \\ 0 & \frac{\nu_\phi}{\alpha_\phi} \end{bmatrix} \begin{bmatrix} \tilde{\alpha}_v \\ \tilde{\alpha}_\phi \end{bmatrix} \\ &\quad + \tilde{\theta}^T \begin{bmatrix} \frac{1}{\alpha_v} & 0 \\ 0 & \frac{1}{\alpha_\phi} \end{bmatrix} \Gamma^{-1} \dot{\tilde{\theta}} \\ &= -W(\chi) - z^T K z, \end{aligned}$$

where the last equality comes from the fact that

$$\dot{\tilde{\theta}} = \Gamma \begin{bmatrix} \nu_v & 0 \\ 0 & \nu_\phi \end{bmatrix} P^T z.$$

As a result, we know that $W(\chi) \to 0$ and $z \to 0$ from Theorem 5.27 in Ref. 18. Note that here $\tilde{\theta}$ may not approach zero.

IV. Simulation Results

In this section, we simulate a small Zagi airframe[19] based UAV that tracks a trajectory generated by a trajectory generator described in Ref. 5. The simulation results in this section are based on a full six degree-of-freedom twelve-state model equipped with low-level autopilots described in Ref. 13. The UAV is equipped with a standard autopilot and the autopilot constants α_* are generally unknown. However, we have tuned the autopilot design to find out that $\alpha_v \approx \frac{1}{2}$ and $\alpha_\phi \approx \frac{1}{0.55}$ for comparison purposes. Table 1 shows the specifications of the UAV and the control law parameters.

Table 1. Specifications of the UAV and the control law parameters.

Parameter	Value
$v_{\min}$	7.5 (m/s)
$v_{\max}$	13.5 (m/s)
$\omega_{\max}$	0.671 (rad/s)
ϕ_{max}	$\frac{\pi}{4}$ (rad)
v_r	$\in [9.5, 11.5]$ (m/s)
ω_r	$\in [-0.471, 0.471]$ (rad/s)
λ	1
η_v	10
η_ω	10
K	diag$\{10, 10\}$
Γ	I

In the first case, we let $v^c = \hat{\alpha}_v \nu_v + v$ and $\phi^c = \hat{\alpha}_\phi \nu_\phi + \phi$, where $\hat{\alpha}_v = \frac{1}{2}$ and $\hat{\alpha}_\phi = \frac{1}{0.55}$. Fig. 1 shows the actual and desired trajectories of the UAV without parameter adaptation. Here we use circles to represent the starting position of the UAV and squares to represent the ending position of the UAV. Also, we use diamonds to represent the position of the UAV at $t = 10, 20, 30, 40$ (secs). It can be seen that the UAV can track its desired trajectory accurately with known α_v and α_ϕ. Fig. 2 shows the tracking error for position and heading. Fig. 3 shows the velocity and roll angle of the UAV. Note that the velocity and roll angle of the UAV satisfy their constraints. The switching phenomena of the roll angle are due to the fact that the reference velocity and heading rate v_r and ω_r are only piecewise continuous.

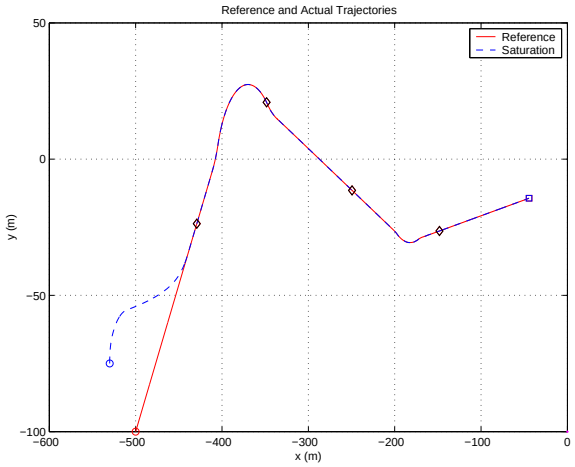

Figure 1. Actual and desired trajectories of the UAV with accurate α_v and α_ϕ but without parameter adaptation.

In the second case, we assume that no parameter adaptation law is applied. Here we let $v^c = \hat{\alpha}_v \nu_v + v$ and $\phi^c = \hat{\alpha}_\phi \nu_\phi + \phi$, where $\hat{\alpha}_v$ and $\hat{\alpha}_\phi$ are arbitrarily chosen as 0.192 and 0.55. Fig. 4 shows the actual and

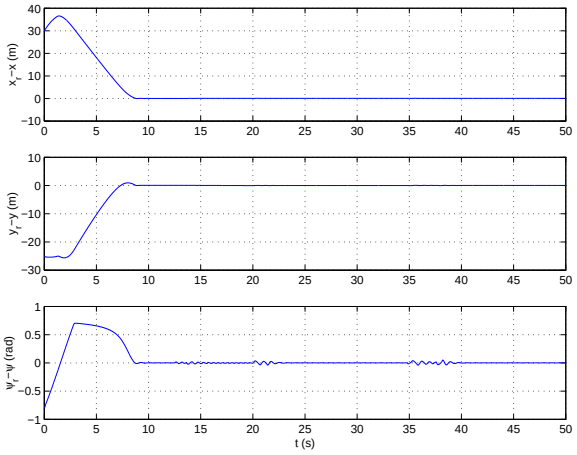

Figure 2. Tracking errors of the UAV with accurate α_v and α_ϕ but without parameter adaptation.

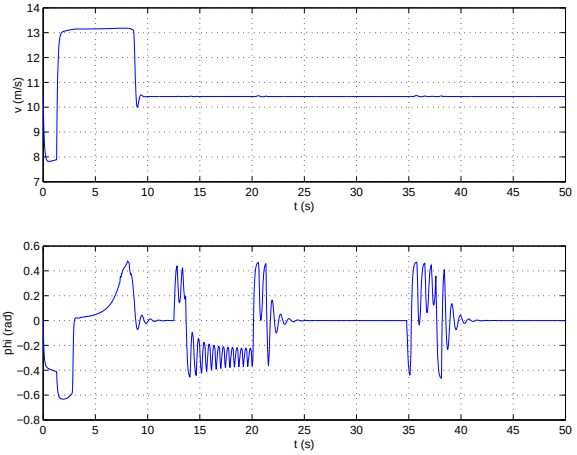

Figure 3. Velocity and roll angle of the UAV with accurate α_v and α_ϕ but without parameter adaptation.

desired trajectories of the UAV with neither accurate α_v and α_ϕ nor parameter adaptation. It can be seen that the UAV cannot track its desired trajectory accurately. Fig. 5 shows the tracking error for position and heading. Fig. 6 shows the velocity and roll angle of the UAV.

In the third case, Eq. (16) is applied to update the estimated parameters $\hat{\alpha}_v$ and $\hat{\alpha}_\phi$, where we assume that $\hat{\alpha}_v(0) = 0.192$ and $\hat{\alpha}_\phi(0) = 0.55$. Fig. 7 shows the actual and desired trajectories of the UAV with inaccurate α_v and α_ϕ but with parameter adaptation. It can be seen that the UAV can track its desired trajectory more accurately in this case than in the second case. Fig. 8 shows the tracking error for position and heading with adaptation. Fig. 9 shows the velocity and roll angle of the UAV with adaptation. Fig. 10 shows the actual and estimated parameters of the UAV. Note that although the estimated parameters do not match the actual parameters here, trajectory tracking errors are still guaranteed to converge to zero due to the inherent properties of adaptive control.[20]

V. Conclusion

With a UAV equipped with low-level autopilots, the twelve-state model of the UAV is reduced to a seven-state model with velocity, roll angle, and altitude command inputs. We have used backstepping techniques to design velocity and roll angle control laws from known velocity and heading angle control laws for small UAVs equipped with effective autopilots. The velocity and roll angle control laws have extended the velocity and heading controllers in Ref. 12, where the velocity and heading controllers explicitly account for limited

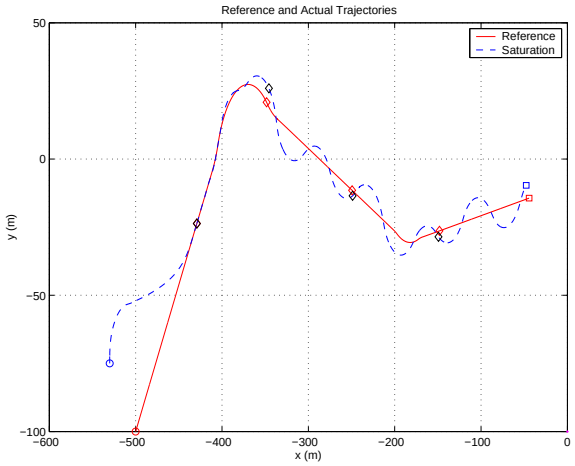

Figure 4. Actual and desired trajectories of the UAV with neither accurate α_v and α_ϕ nor parameter adaptation.

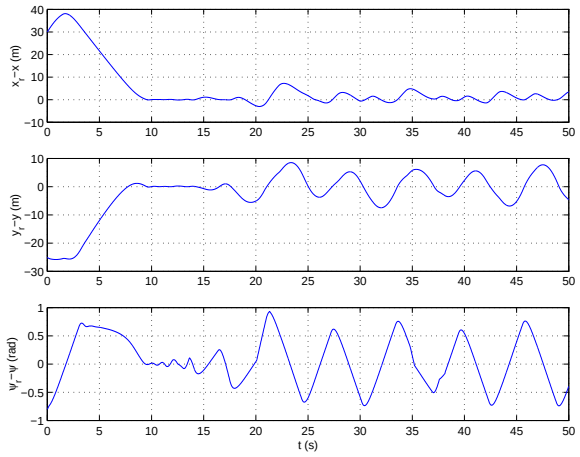

Figure 5. Tracking errors of the UAV with neither accurate α_v and α_ϕ nor parameter adaptation.

velocity and heading rate constraints of fixed wing UAVs. A parameter adaptation technique has been applied to estimate unknown autopilot parameters. Simulation results on a small fixed wing UAV have shown the effectiveness of our approach.

Acknowledgments

The authors would like to gratefully acknowledge Prof. Randy Beard and Derek Kingston from Brigham Young University for discussing the ideas of this paper.

References

[1]Clough, B. T., "Unmanned Air Vehicles: Autonomous Control Challenges, A Researcher's Perspective," *Cooperative Control and Optimization*, edited by R. Murphey and P. M. Pardalos, Vol. 66, Kluwer Academic Publishers Series: Applied Optimization, 2002, pp. 35–53.

[2]Bortoff, S. A., "Path Planning for UAVs," *Proceedings of the American Control Conference*, 2000.

[3]Chandler, P., Rasumussen, S., and Pachter, M., "UAV Cooperative Path Planning," *Proceedings of the AIAA Guidance, Navigation, and Control Conference*, Denver, CO, August 2000, AIAA Paper No. AIAA-2000-4370.

[4]Yakimenko, O. A., "Direct Method for Rapid Prototyping of Near-Optimal Aircraft Trajectories," *AIAA Journal of Guidance, Control, and Dynamics*, Vol. 23, No. 5, September-October 2000, pp. 865–875.

[5]Anderson, E. P. and Beard, R. W., "An Algorithmic Implementation of Constrained Extremal Control for UAVs,"

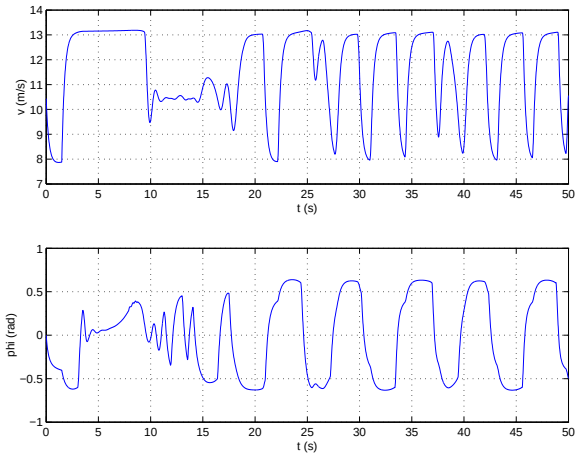

Figure 6. Velocity and roll angle of the UAV with neither accurate α_v and α_ϕ nor parameter adaptation.

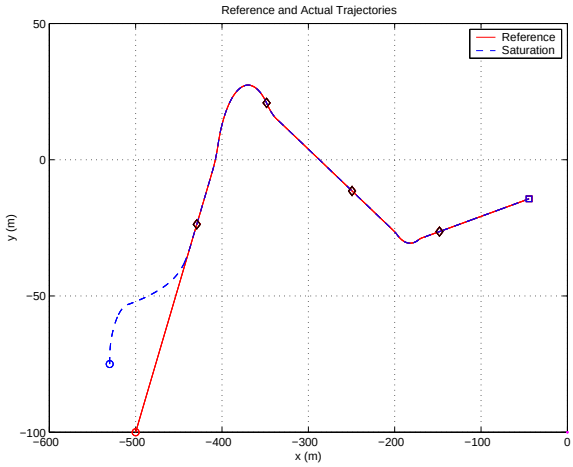

Figure 7. Actual and desired trajectories of the UAV with inaccurate α_v and α_ϕ but with parameter adaptation.

Proceedings of the AIAA Guidance, Navigation, and Control Conference, Monterey, CA, August 2002, Paper no. AIAA-2002-4470.

[6]McLain, T. W. and Beard, R. W., "Cooperative Rendezvous of Multiple Unmanned Air Vehicles," *Proceedings of the AIAA Guidance, Navigation and Control Conference*, Denver, CO, August 2000, Paper no. AIAA-2000-4369.

[7]Kang, W. and Sparks, A., "Task Assignment in the Cooperative Control of Multiple UAVs," *Proceedings of the AIAA Guidance, Navigation, and Control Conference*, Austin, TX, August 2003, Paper no. AIAA-2003-5583.

[8]Chandler, P. R., "Cooperative Control of a Team of UAVs for Tactical Missions," *AIAA 1st Intelligent Systems Technical Conference*, Chicago, IL, September 2004, Paper no. AIAA-2004-6215.

[9]McLain, T. W. and Beard, R. W., "Coordination Variables, Coordination Functions, and Cooperative Timing Missions," *AIAA Journal of Guidance, Control, and Dynamics*, 2004, (to appear).

[10]Beard, R. W., McLain, T. W., Goodrich, M., and Anderson, E. P., "Coordinated Target Assignment and Intercept for Unmanned Air Vehicles," *IEEE Transactions on Robotics and Automation*, Vol. 18, No. 6, 2002, pp. 911–922.

[11]Beard, R. W., Lawton, J. R., and Hadaegh, F. Y., "A Coordination Architecture for Formation Control," *IEEE Transactions on Control Systems Technology*, Vol. 9, No. 6, November 2001, pp. 777–790.

[12]Ren, W. and Beard, R. W., "Trajectory Tracking for Unmanned Air Vehicles with Velocity and Heading Rate Constraints," *IEEE Transactions on Control Systems Technology*, Vol. 12, No. 5, September 2004, pp. 706–716.

[13]Kingston, D., Beard, R., McLain, T., Larsen, M., and Ren, W., "Autonomous Vehicle Technologies for Small Fixed Wing UAVs," *AIAA 2nd Unmanned Unlimited Systems, Technologies, and Operations–Aerospace, Land, and Sea Conference and Workshop & Exhibit*, San Diego, CA, September 2003, Paper no. AIAA-2003-6559.

[14]Proud, A. W., Pachter, M., and D'Azzo, J. J., "Close Formation Flight Control," *Proceedings of the AIAA Guidance, Navigation, and Control Conference*, Portland, OR, August 1999, pp. 1231–1246, Paper No. AIAA-99-4207.

[15]Kanayama, Y. J., Kimura, Y., Miyazaki, F., and Noguchi, T., "A stable tracking control method for an autonomous mobile robot," *Proceedings of the IEEE International Conference on Robotics and Automation*, 1990, pp. 384–389.

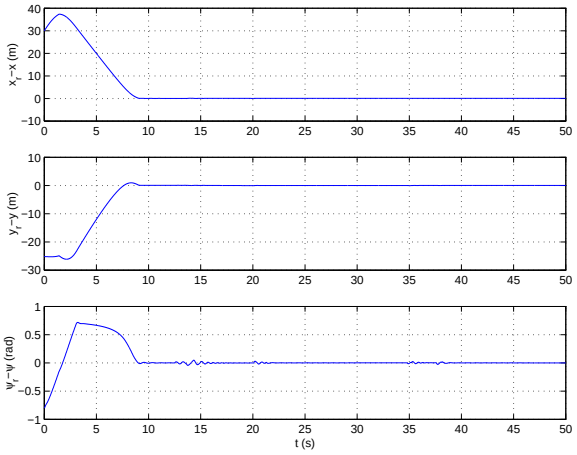

Figure 8. Tracking errors of the UAV with inaccurate α_v and α_ϕ but with parameter adaptation.

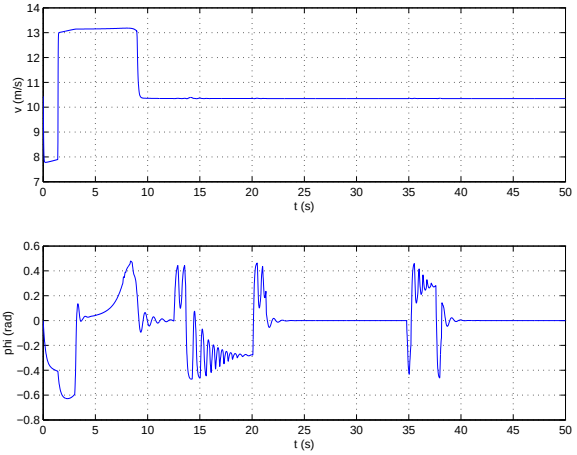

Figure 9. Velocity and roll angle of the UAV with inaccurate α_v and α_ϕ but with parameter adaptation.

[16]Shevitz, D. and Paden, B., "Lyapunov Stability Theory of Nonsmooth Systems," *IEEE Transactions on Automatic Control*, Vol. 39, No. 9, 1994, pp. 1910–1914.

[17]Tanner, H. G. and Kyriakopoulos, K. J., "Backstepping for Nonsmooth Systems," *Automatica*, Vol. 39, 2003, pp. 1259–1265.

[18]Sastry, S., *Nonlinear Systems Analysis, Stability, and Control*, Springer-Verlag, New York, 1999.

[19]http://zagi.com.

[20]Slotine, J.-J. E. and Li, W., *Applied Nonlinear Control*, Prentice Hall, Englewood Cliffs, New Jersey, 1991.

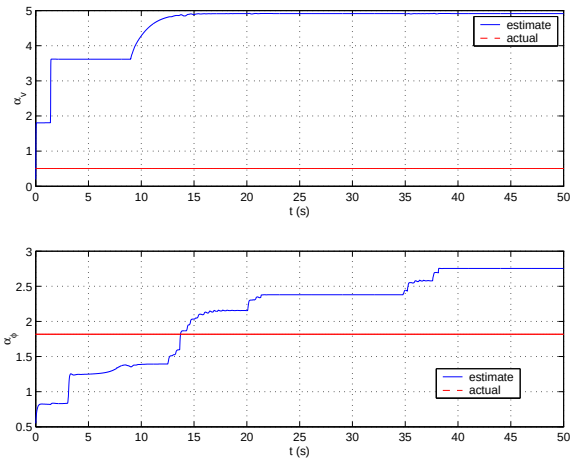

Figure 10. Parameter estimates of the UAV with inaccurate α_v and α_ϕ but with parameter adaptation.